Materials and Design 193 (2020) 108873

Contents lists available at ScienceDirect

Materials and Design

journal homepage: www.elsevier.com/locate/matdes

A critical assessment of experimental investigation of dynamic recrystallization of metallic materials

H.K. Zhang [a], H. Xiao [a], X.W. Fang [a], Q. Zhang [a], R.E. Logé [b], K. Huang [a,c,*]

[a] State Key Laboratory for Manufacturing Systems Engineering, School of Mechanical Engineering, Xi'an Jiaotong University, Xi'an 710049, Shaanxi, PR China
[b] Thermomechanical Metallurgy Laboratory – PX Group Chair, Ecole Polytechnique Fédérale de Lausanne (EPFL), CH-2002 Neuchâtel, Switzerland
[c] National Key Laboratory for Precision Hot Processing of Metals, Harbin Institute of Technology, Harbin 150001, PR China

HIGHLIGHTS

- Common dynamic recrystallization (DRX) mechanisms are reviewed.
- The disturbing effect of strain localization on DRX is discussed.
- The neglected post DRX after hot deformation is examined.
- The possible phase transformation during and after hot deformation is considered.

GRAPHICAL ABSTRACT

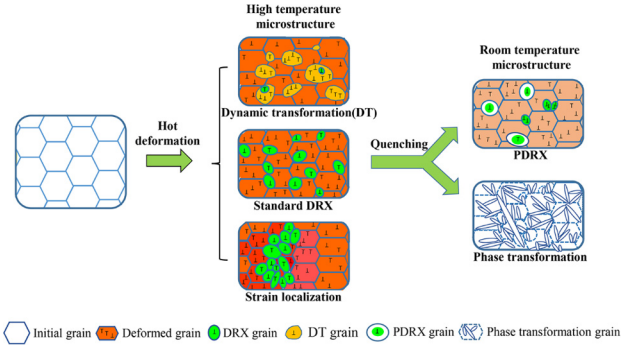

ARTICLE INFO

Article history:
Received 6 December 2019
Received in revised form 5 June 2020
Accepted 7 June 2020
Available online 8 June 2020

Keywords:
Dynamic recrystallization
Post dynamic recrystallization
Strain localization
Phase transformation
Dynamic transformation

ABSTRACT

Dynamic recrystallization (DRX) often takes place during hot deformation of metallic materials, which then exerts significant influence on the final microstructures and mechanical properties of the formed components. A considerable number of published papers related to DRX, however, suffer from non-negligible flaws originating from inappropriate experimental design. In this paper, the sources of these flaws are critically assessed, including the misinterpretation of DRX mechanisms, the strain localization on tested samples, the neglected post dynamic recrystallization and possible phase transformations which mask the real hot deformation microstructure. Solutions to eliminate or quantify these disturbing factors during DRX studies are suggested, yielding more accurate approaches to investigate DRX behaviour of metallic materials.

Contents

* Corresponding author at: State Key Laboratory for Manufacturing Systems Engineering, School of Mechanical Engineering, Xi'an Jiaotong University, Xi'an 710049, Shaanxi, PR China.
E-mail address: ke.huang@xjtu.edu.cn (K. Huang).

https://doi.org/10.1016/j.matdes.2020.108873

1. Introduction

Dynamic recrystallization (DRX), which takes place during hot deformation of metallic materials once a critical strain level has been reached, can significantly modify the microstructures and mechanical properties of the formed component [1]. Since the 1940s, extensive investigation has been invested on the development of DRX theory [2], focusing mainly on the two most widely used structural alloys, i.e., steels and aluminium alloys. The three typical DRX mechanisms, including discontinuous dynamic recrystallization (DDRX), continuous dynamic recrystallization (CDRX) and geometric dynamic recrystallization (GDRX) have been summarized in recent review papers [3,4]. Driven by the fast development of new metallic materials, especially those with low ductility that have to be deformed at high temperatures, DRX has now become a relatively hot research topic, as reflected by the large number of published papers, as well as its fast-growing speed (see Fig. 1).

It appears that the relatively well-developed knowledge of DRX in steels and aluminium alloys is often vaguely applied to hot working of other new metallic materials, e.g., titanium alloys, magnesium alloys, high entropy alloys etc. For instance, CDRX was often claimed to occur without direct proofs of the gradual evolution of low angle grain boundary (LAGB) misorientation angle distributions. GDRX was used to explain the formation of small grains during hot deformation at very small strain levels, neglecting the fact that the critical strain for GDRX is usually very large. Meanwhile, most DRX studies are performed by examining the post-mortem microstructures preserved by quenching after deformation. Strain localization, which not only changes the local strain levels, but also modifies the local strain rate, is often unnoticed if DRX analysis is conducted in this fashion. Quench delay and possible phase transformation (e.g., titanium alloys, steels) during cooling mask the hot deformation structure, adding difficulties to the DRX analysis. In order to get an in-depth understanding of the DRX behaviour and to quantitatively tailor the final hot deformation microstructure, solutions to resolve the above-mentioned issues are required.

Numerical modelling provides an alternative way for studying DRX at different length scales, but for the sake of simplicity, the following discussion will be restricted to experimental aspects of DRX. Interested readers are referred to Refs [4–7] for more details on modelling of DRX. In fact, the development of more advanced DRX models relies heavily on the accumulation of systematic and accurate experimental data, which is the focus of the current paper. This paper also reviews critically the origins of non-rigorous interpretations of high temperature DRX experiments and suggests solutions to avoid them.

2. DRX mechanism

2.1. Common DRX mechanisms and existing problems

During hot deformation of metallic materials with low stacking fault energy (SFE), DDRX takes place, through two distinct stages, i.e. nucleation and growth of the nuclei, once a critical strain has been reached. The characteristics of DDRX have been well established in textbooks [1] and recent review papers [3–5]. Since other DRX mechanisms are less present in the literature, DDRX is often interchanged with DRX. During DDRX, dislocation-free nuclei are firstly formed at a serrated boundary, which then leads to necklace-type small recrystallized grains along the original grain boundaries (GBs) at larger strain levels. This has been the focus of numerous studies, however, much less investigations can be found on the progress of DRX after the formation of the first necklace. The role of twinning in promoting nucleation of new grains during DDRX was, in particular, evidenced in Refs [8–10].

It is often taken for granted that DDRX will definitely lead to grain refinement, however, grain coarsening could easily take place under certain conditions. Fig. 2a illustrates the grain size changes of pure nickel with different initial grain size during hot working [3]. After DDRX, the average grain size of the sample with a coarser initial grain size of 60 μm indeed decreases to around 40 μm, but the increased average grain size is also evident for the sample with smaller initial grain size of 30 μm. The mechanism behind is actually easy to follow: since the steady state grain size is a function of deformation temperature and strain rate, deformation of materials with small initial grain size at high temperature with low strain rate could easily lead to a coarser grain structure. The type of flow stress curve may also change from single peak to multiple peak when decreasing the initial grain size [11], see Fig. 2b.

Even though aluminium alloys are important structural materials and hot rolling is a standard processing step in industrial practice, the corresponding DRX behaviour is still under debate [12,13]. The microstructure evolution of Al alloys through CDRX was put forward by Perdrix et al. in 1981 [14]. CDRX originally refers to the microstructure evolution by progressive transformation of LAGBs into high angle grain boundaries (HAGBs). However, in standard forming operations (hot forging, hot rolling and extrusion, etc.) of Al alloys, complete CDRX is rarely observed due to the presence of stable grains [13], the misorientation of LAGBs in stable grains does not steadily increase even after large strain (as shown in Fig. 3) [12,15–19]. The deformation behaviour of these stable grains should definitely be further investigated. Three different forms of CDRX mechanisms were proposed in Refs [4], including CDRX by the homogeneous increase of misorientation (HIM), CDRX by lattice

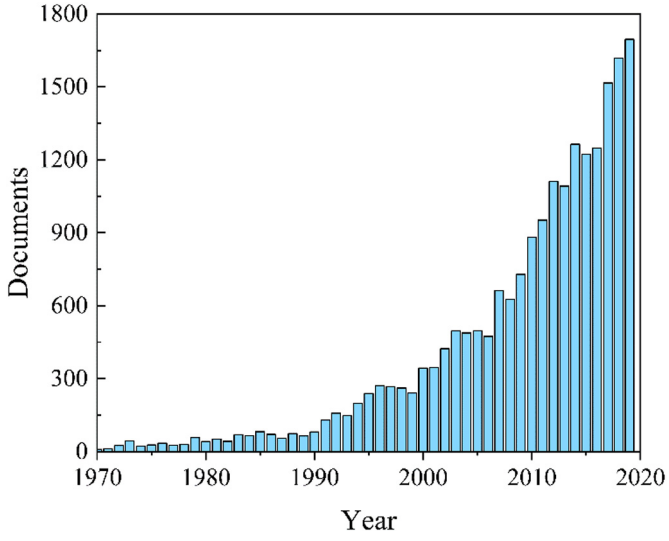

Fig. 1. The fast-growing number of published papers related to DRX from 1970 to 2019. Data from Web of Knowledge with "dynamic recrystallization" as "Topic" on May 26, 2020.

rotation near grain boundary (LRGB), as well microshear band assisted CDRX.

GDRX refers to the formation of equiaxed grains during hot deformation by the following three steps: 1) formation of serrations; 2) grain elongation and thinning; 3) impingement of serrated original HAGBs at critical strain. Solberg and McQueen, together with their co-workers, were the first ones to use the term GDRX [20,21]. The GDRX mechanism is only based on geometrical considerations. It is indeed true that GDRX begins earlier near triple junctions where the distance between the HAGBs is smaller, but the critical strain, which depends on the deformation mode, subgrain size and initial grain size, must be reached before substantial GDRX takes place. For metallic materials with typical initial grain size of ~50-100 μm, this critical strain is much higher than the reachable uniform deformation strain in hot tension or compression tests. Moreover, the introduction of new HAGBs by grain subdivision or transformed LAGBs during deformation should be distinguished from the original HAGBs when interpreting GDRX.

2.2. New DRX mechanism and its applicability

Besides the three typical DRX mechanisms, twinning-induced DRX (TDRX) has been reported extensively in magnesium and its alloys [22–26]. During TDRX, the new grains first nucleate in twins and at twin-twin intersections (Fig. 4) [23,27,28], the twin boundaries then change into ordinary boundaries, and these grains then finally grow [29]. Although few reports have been documented in high temperature ranges [30,31], the TDRX mechanism plays an important role in the deformation of magnesium and its alloys [32,33]. However, it is rarely reported in materials other than magnesium alloys.

DRX is usually a thermally activated process and a minimum temperature is required to initiate associate atomic mechanisms. Disclination mediated DRX, which can operate at temperature as low as $T = 10$ K in metallic materials during deformation, was put forward through atomic simulation [34]. Different from dislocation-based models, this mechanism relies on the formation of special defects of disclination quadrupoles, which take place during deformation in case where the grain boundary migration is restricted by structural defects such as triple junctions, cracks or obstacles. Since the focus of this paper is placed on the experimental study of DRX, the disclination mediated DRX study by atomic simulation will thus not be further discussed, interested readers are referred to Refs [34, 35] for more details.

Heteroepitaxial recrystallization (HERX), which was firstly reported in nickel-based superalloys with a large volume fraction of second-phase particles [36,37], takes place when a γ shell is formed coherently on the primary precipitates γ′ prior to the deformation and this γ shell serves as recrystallization nucleus during deformation while maintaining its coherency with the primary γ′ (shown in Fig. 5) [37]. However, although HERX is intensified at low temperature and high strain rates, HERX grains will gradually be replaced by DDRX grains under large strain [38]. Therefore, HERX can be considered as a special case of the early stages of DDRX or as an auxiliary mechanism for DDRX under low strain. The HERX mechanism is only likely to occur in low lattice mismatch superalloys since it is a necessary condition for the development of such large heteroepitaxial features [37].

In addition, some "new" mechanisms such as rotational dynamic recrystallization (RDRX) [39–41], grain boundary bulging dynamic recrystallization (GBBDRX) [33,42,43], low-temperature dynamic recrystallization (LTDRX) [44,45] have been reported, but these mechanisms are either similar to existing DRX mechanisms or are often limited to specific materials or deformation volumes.

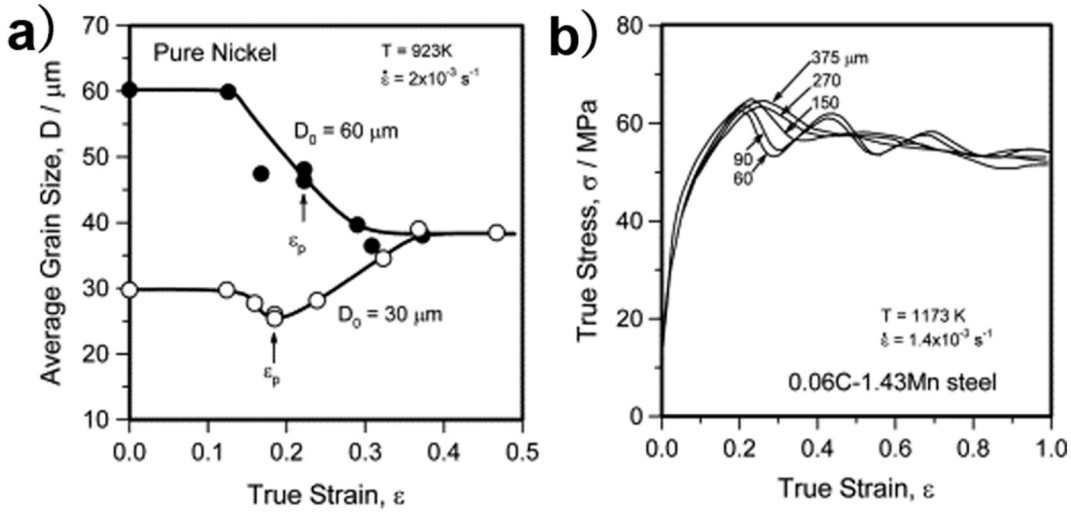

Fig. 2. a) Average grain size change of pure nickel in DDRX [3]. b) Typical stress-strain curves characteristic of DDRX in the austenite of plain carbon steels [11]. Reprinted with permission from Elsevier [3,11].

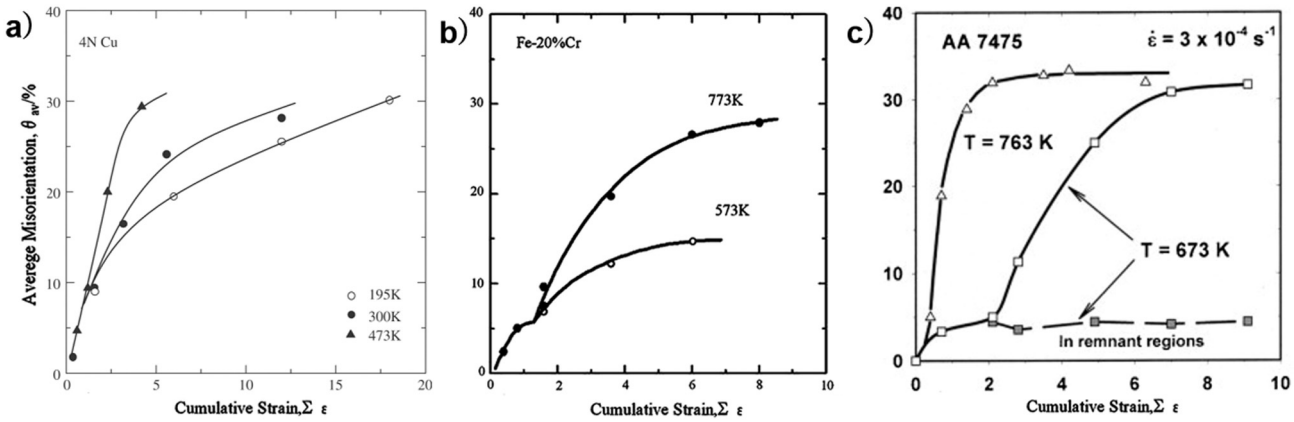

Fig. 3. The change in average misorientation angle with strain for a) Cu [3,17], b) Fe-20% Cr alloy [3,18] and c) AA7475 [3,19] undergoing CDRX. Reproduced with permission from Elsevier [3].

2.3. Multiple mechanisms operate sequentially or simultaneously

Now that typical individual DRX mechanisms have been reviewed in the previous sections, we can turn to more complex situations where the hot deformation of metallic materials involves more than one DRX mechanism. Different DRX mechanisms can operate in sequence or in parallel [23,27,33,39–41,46–51].

The change of DRX mechanism with respect to deformation strain, deformation temperature and strain rate is well documented in magnesium alloys [33,45], steels [52,53] and nickel alloys (Fig. 6) [48–50]. On the other hand, the simultaneous operation of different DRX mechanisms is a more complex situation. Although a large number of experiments have found that different mechanisms could operate synchronously [46,50,51], it remains a difficult task to separate different DRX mechanisms. For instance, HAGBs can be formed by CDRX during hot deformation, which reduces the distances between HAGBs and triggers "GDRX" (only original HAGBs are considered during traditional GDRX) at small strain levels (typically <1). It is almost impossible to judge the DRX mechanism just by looking at the final microstructure and the flow stress curve, especially when multiple DRX mechanisms are involved. Moreover, the complex interaction between DRX and phase transformation (and also second-phase particles) further makes it difficult to analyse the real DRX mechanism for many metallic materials. Careful results analysis is required before jumping into conclusions.

In order to separate different DRX mechanisms, the microstructure evolution with respect to strain, which provides the gradual microstructure evolution, should always be investigated. The microstructure evolution should be ideally tracked by 3D in-situ methods. However, even though a few techniques such as laser ultrasonics [54] and in-situ high energy synchrotron radiation diffraction have indeed been attempted [55]. Most of them are targeted on the average state variables such as crystallite size and dislocation density, whereas the direct monitoring of the microstructure evolution of individual grains is still unavailable. The microstructure evolution can also be in-situ tracked on the 2D free surface during hot deformation within the SEM chamber [56], but the reachable strain level is limited due to the severe deformation on the surface. It thus appears that post-mortem microstructure analysis is still the right approach to distinguish the concurrent DRX mechanisms. DDRX usually takes place for materials with low SFE and it is characterized by the early nuclei initiated at original GBs with almost dislocation-free internal structure which then suffers to subsequent deformation. A necklace grain structure can be observed after the peak strain, while twinning plays a role when the original GBs are consumed [57]. It should be noted that both grain refinement and grain coarsening are possible depending on the deformation conditions [3,4]. To identify the CDRX, the progressive evolution of the misorientation angle distribution should always be given, since this provides the key evidence for *traditional* CDRX. Before the completion of CDRX, the new potential grains formed by this mechanism should be surrounded by LAGBs with a range of misorientation angles up to 10-15°. A gradual increase in the misorientations between prospective grains is accompanied by the formation of grain/subgrain boundary net consisting of LAGBs and HAGBs. Corresponding structural elements, i.e., grains and/or subgrains, in such microstructure are partially bounded by LAGBs and HAGBs, and the fraction of the latter ones increases upon CDRX progress [3]. In contrast to DDRX, CDRX is characterized by rather homogeneous dislocation substructure evolution during deformation, which is another common distinctive feature of continuous processes [1,3]. Since new grains during CDRX form in place of deformation subgrains as a result

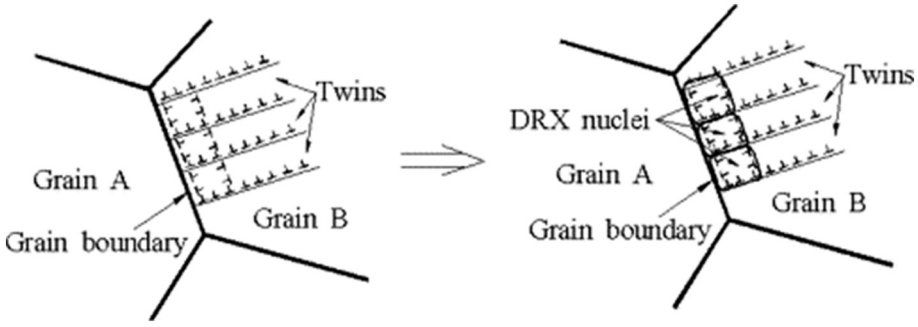

Fig. 4. Schematic representation of the TDRX mechanism [28]. Reproduced with permission from Elsevier [28].

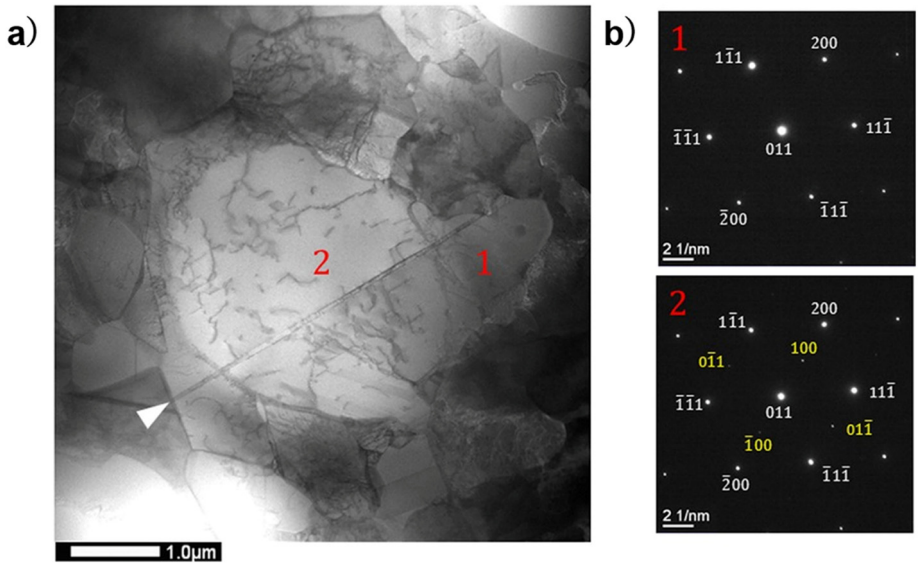

Fig. 5. a) STEM image of a primary precipitate surrounded by a γ grain. b) Selected area diffraction patterns in [110] zone axis, corresponding to the γ grain 1 and the γ′ precipitate 2 [37]. Reproduced with permission from Wiley [37].

of increasing sub-boundary misorientations, the dislocation density should depend on deformation conditions, but being nearly the same in all grains/subgrains.

The formation of HAGBs due to progressive lattice rotation near GBs and the microshear band has been regarded as non-traditional CDRX [4], and the generation of strong texture under large strain can be an auxiliary criterion for CDRX [4,19]. CDRX prevails for materials with high SFE, but it has been evidenced in low SFE materials under warm deformation conditions [48]. Depending on the deformation mode, some stable orientations, within which the average misorientation angle saturates below 10°, may still exist even at very high strain levels [3], this should not be taken as an evidence to exclude CDRX. The judgment of GDRX is theoretically simple but still requires attention due to its similarities with CDRX, it was even classified as one special case of CDRX [1]. The critical strain, which is usually much higher than the attainable strain during hot compression and tension, should be reached if the majority of the materials is recrystallized by CDRX. Of course, the critical strain will be much smaller at the acute ends of irregular grains, but this only accounts for a limited fraction of the total GBs [4,21]. A good and simple way to avoid GDRX is obviously to increase the initial grain size of the investigated material.

In additional to the post-mortem microstructure analysis, knowing the SFE of the investigated material, as well as analysing its stress-strain curves at different conditions up to large strain levels may also help to distinguish different DRX mechanisms. For instance, dynamic recovery in high SFE materials promotes dislocation redistribution during deformation that is accompanied by a gradual increase in the flow stress approaching a saturation at large strain. DDRX is rarely observed for aluminium alloys (except pure aluminium) which possess high SFE, but stress-strain curve with evident peak (or even multiple peaks) followed by a steady state plateau suggests DDRX since stress peak is usually not seen for both GDRX and CDRX.

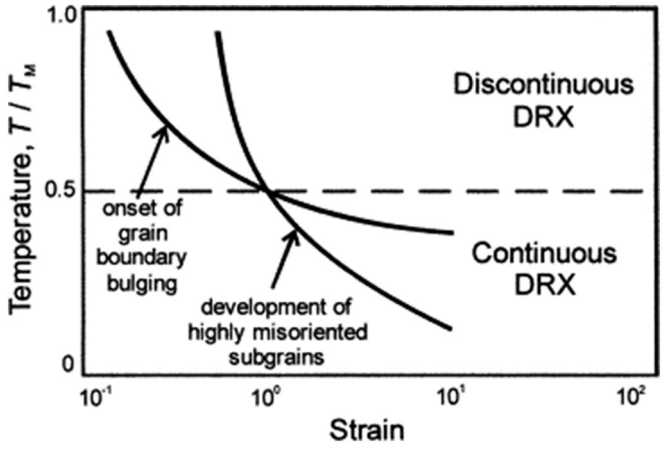

Fig. 6. Schematic drawing showing the various DRX mechanisms responsible for new grain development during plastic working of Ni-20%Cr alloy [48].
Reproduced with permission from Elsevier [48].

3. Strain localization

3.1. Sources leading to strain localization

Strain localization refers to the narrow zone of larger-than-average strain on the deformed sample, with necking being one of the typical examples. Strain localization not only leads to the increased strain level in that particular zone, it also affects the corresponding strain rate, both of which have a significant role on the DRX behaviour of the material. Even though the accumulated strain level can be estimated in the strain localized area, it is much more difficult to estimate the history of strain rate.

Temperature gradients along the tested samples are one of the most common sources of macroscopic strain localization during hot deformation. Localized deformation heating further promotes temperature gradients and strain localization [58]. During a hot tensile test, for example, there is, at sufficient strain rates, a significant temperature rise in the necking zone [59]. Sample-anvil friction during compression test is one of the main causes of inhomogeneous strain in this type of test, which causes changes in metal flow characteristics [60,61]. Strain localization near the surface of the rolled sheets by strong shear deformation is frequently observed during hot rolling due to the friction between the rolls and the sheets. Friction between billet and die also leads to dead metal zone and shear zone during extrusion. The geometric parameters of the sample, including those induced by machining, are also influencing factors of strain localization, which are analysed in detail in Refs [61–63]. Deformable second-phase particles in the metallic matrix can, on the other hand, also result in or increase microscopic strain

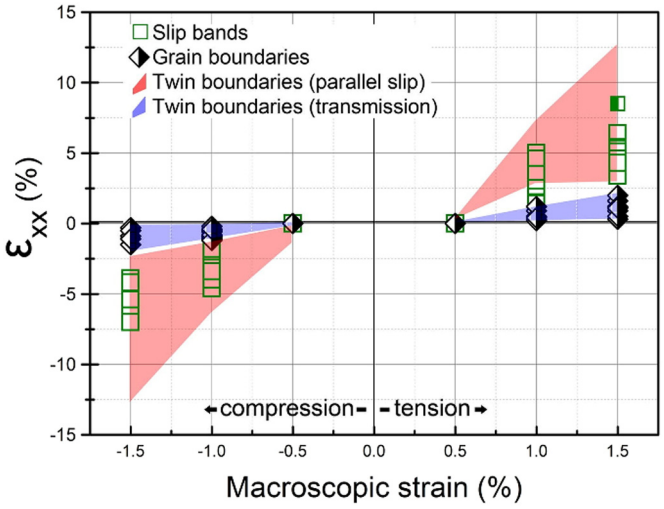

Fig. 7. Average strain accumulation along slip bands (excluding strain accumulation at bands within 1 μm of twin boundaries) and grains boundaries (excluding twin boundaries) in tension and compression tests on René 88DT polycrystalline nickel-based superalloy.
Reproduced with permission from Elsevier [69].

localization, e.g. through the formation of shear bands. For example, strain localization almost doubled when introducing very fine and coherent Ti_3Al (α_2) precipitates in Ti-6Al-4 V alloys [64–66]. In general, strain localization occurs preferentially near grain boundaries and twin boundaries (as illustrated in Fig. 7) due to the lack of efficient mechanisms for strain transfer across such interfaces [67–70]. In addition, the constraint imposed by neighboring grains also leads to strain localization [71]. Inversely to strain localization, stable grains, which do not transform into smaller grains even after very high strain level, are frequently observed during hot deformation of Al alloys [3,4].

3.2. Methods for determining strain localization

In common deformation experiments of DRX studies such as hot tensile, compression and torsion tests, a practical way to measure potential strain localization is to examine the final shape of the deformed sample. During hot torsion, it is enough to draw a shallow but straight line on the gauge length of the sample with a sharp tool before the test. After deformation, the spacing between the spiral lines should be uniform in the case of homogeneous deformation. Attention should be paid on the rough surface either due to orange peel effect (see Fig. 8) [72], related to a large initial grain size, or scales caused by oxidation, since both of them can make the marked line invisible after deformation. Under hot compression, the friction between the sample and the anvils leads to a non-uniform strain. However, comparing the final shape of the deformed sample with that simulated by finite element analysis (FEA) under homogeneous temperature can be used to quantify strain localization in 3D. During hot tension, in addition to visually observing obvious strain localization such as necking, strain distribution can be determined within a certain range by Digital Image Correlation (DIC), or simply by analysing the stress-strain curve using the Considère criterion [73].

Recently, High Resolution Digital Image Correlation (HRDIC) has been used to quantify microscopic strain localization in multiple experiments [65,69,71,74]. As shown in Fig. 9, since the spatial resolution is then at the μm-scale, this method provides highly resolved strain information. The specific strain level of the deformation zone can be clearly presented, and the different strains can be accurately quantified [74]. However, this technique has many drawbacks, including the small analysed area and the complex data smoothing procedure etc., as detailed in Ref [75].

3.3. Elimination or reduction of strain localization

Once strain localization is quantified, methods should be proposed to avoid it. The essence of strain localization is the inhomogeneity of metal plastic flow. First, uniform temperature distribution is the most important factor to avoid strain localization. The temperature along the deformation section of the tested samples should be kept as homogeneous as possible. This can be carried out by long soaking time, smooth transition zone between the gauge section and sample shoulders for tensile and torsion tests. It should be noted that long soaking time can generally make the temperature of the sample more uniform, but it may have limited effect at extremely high deformation temperature (>1000 °C). It is highly recommended to install thermocouples in different parts of the sample to monitor the temperature uniformity whenever it allows. Since the deformation heating becomes more significant at high strain rates, and an increase of strain rate tends to change the conditions from isothermal to adiabatic, deformation at lower strain rate is recommended as long as it is allowed, in order to avoid additional strain induced temperature gradients [76].

It is also an effective method to choose the appropriate deformation conditions in terms of deformation temperature and strain rate

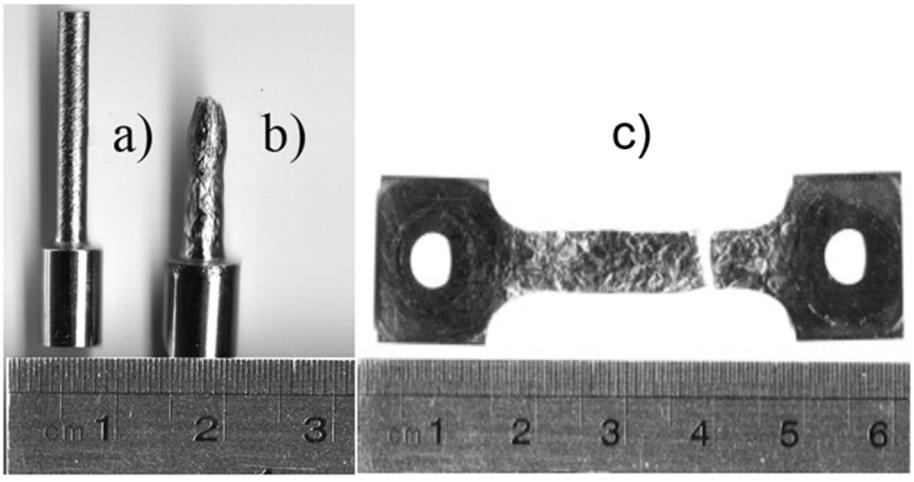

Fig. 8. Wrinkling on the surface of a) a torsion sample, b) a cylindrical tensile sample, and c) a flat square type tensile sample after fracture.
Reprinted with permission from Elsevier [72].

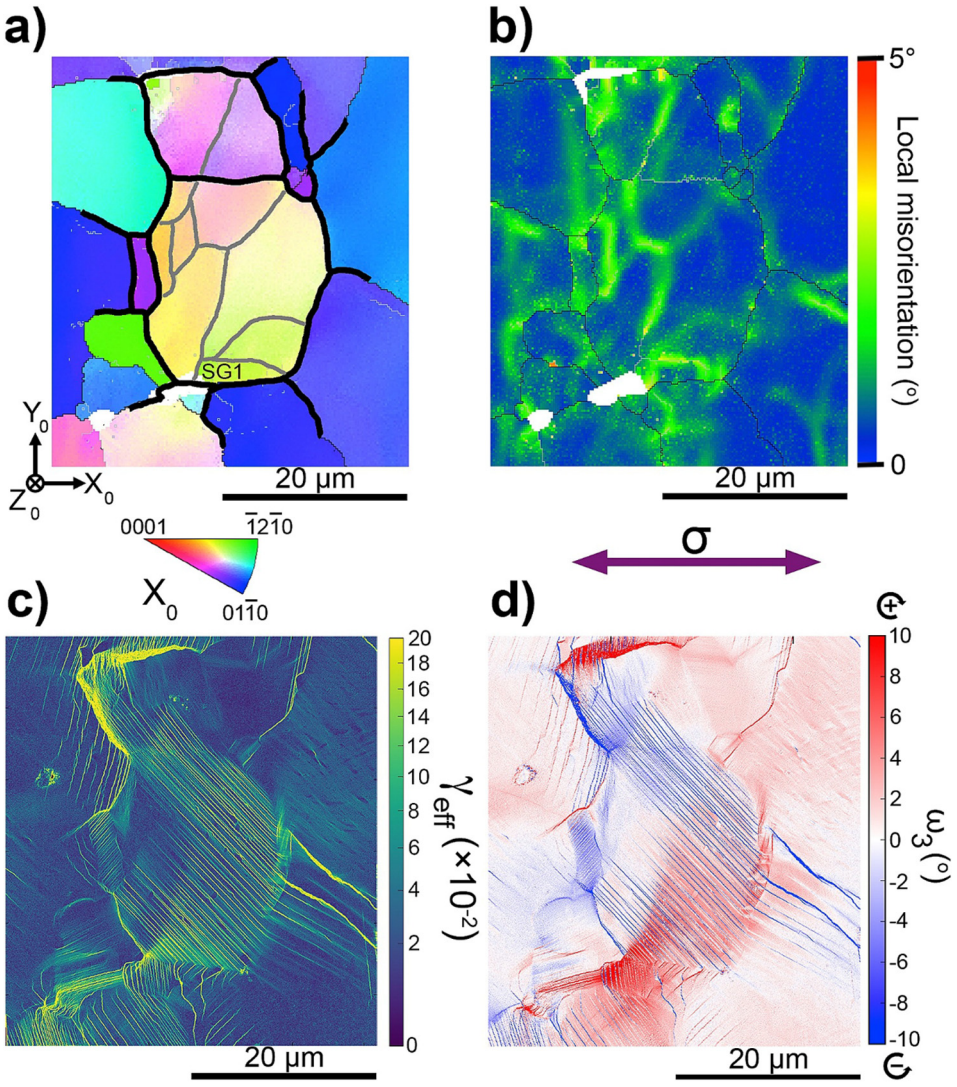

Fig. 9. Detailed analysis of grain breaking process of magnesium alloy by EBSD and HRDIC. a) EBSD map represented using IPF colours respect to the loading direction (X0) including a schematic of the grain boundaries in black (2° ≤ misorientation <15°) and the subgrain boundaries in grey (misorientation ≥15°), b) local misorientation or KAM (kernel average misorientation) map using a 9 × 9 kernel size, c) effective shear strain values showing the intensity and localization of different slip events and d) ω3 (the amount of rigid body rotation about normal plane x3) values showing the rigid body rotation between slip bands is similar to the crystallographic rotations observed [74].
Reprinted with permission from Elsevier [74].

(which can be jointly considered through the Zener-Hollomon parameter), according to the material processing map [77,78]. For instance, deforming at a condition with a low strain rate sensitivity value usually leads to strain localization [77]. According to the Considère criterion for tensile test, strain localization on a macroscopic scale, such as necking, may be delayed by increasing the work hardening rate which then promote large uniform plastic deformation [79,80]. In terms of deformation mode, torsion testing is particularly appropriate for large deformation testing at high temperatures, since a constant cross section is maintained throughout the test. Using proper lubrication, true stress-strain curves can also be obtained and analysed after compression tests, but this usually only holds true when the true strain is <1.0. It should be noted that possible strain heterogeneity is easily controlled by the shape of compressed specimen.

In general, samples with good surface finish and smooth geometrical transitions help reducing strain localization during hot deformation. However, it was reported that compression samples with concentric shallow grooves (i.e. rough surface) on both ends lead to more homogeneous deformation since they help keeping a sufficient amount of lubricant during hot deformation [81]. At the same time, lubricants such as graphite, powdered glass and mixtures of powdered glass and boron nitride powder should be selected differently depending on the material and deformation conditions [81]. Finally, the uniformity of (micro)chemical composition and microstructure of the deformed sample should be ensured as much as possible, proper homogenization treatment and examination of the initial microstructure are necessary before hot deformation.

4. Post dynamic recrystallization (PDRX)

4.1. Characteristics of PDRX

PDRX, also known as metadynamic recrystallization (MDRX), occurs once deformation stops while deformation temperature does not drop sufficiently fast. The freshly nucleated DDRX grains then continue to grow without requiring an incubation time [2,82–86]. Even though PDRX is not a new phenomenon, it has been often neglected, sometimes resulting in ungrounded conclusions. PDRX could take place extremely fast, especially after hot deformation

conditions with very high temperatures and large strain rates. The onset of PDRX significantly modifies the deformation microstructure, leading to a complex mixture of original deformed grains, dynamically recrystallized grains with subsequent strain-hardening, and fresh DRX grains that have grown by PDRX. Fast PDRX kinetics is illustrated in Fig. 10, where a hot deformed nickel sample was quenched by hydrogen gas after holding at the deformation temperature for 0.03 s, which was not sufficient to prevent PDRX. The development of dislocation density distributions in PDRX microstructures was analysed in Ref [3, 83]. During PDRX, another central question is whether SRX could still take place when the deformation stops but the temperature is kept high. It is often claimed that PDRX is the only softening mechanism, both from experimental studies [83] and numerical simulations [87,88]. However, in a recent study using in situ characterization of Inconel 718, it was found that SRX could still take place in addition to PDRX, as long as the initial dynamically recrystallized volume fraction is low enough [89]. Even though PDRX should usually be avoided in DRX studies since it masks the deformation microstructure, it can also be intentionally used to tailor the final microstructure. In fact, PDRX is difficult to avoid in many industrial practices when very large ingots are hot deformed under multi-pass conditions. It is even more so for metallic materials with low thermal conductivities. Even though not related to PDRX, attention should also be paid to the possible SRX when heating samples with an initial deformation microstructure.

4.2. Assessment and controlling of PDRX

The fast kinetics of PDRX discussed in Section 4.1 requires appropriate quantification methods. The double-hit experiment, consisting of two separate deformation stages, is considered to be an effective method for assessing PDRX [90]. According to the stress-strain curve of the double-hit isothermal experiment, the degree of softening caused by PDRX during two hit intervals can be quantified through the notion of softening fraction [86]:

$$X_s = \frac{\sigma_3 - \sigma_1}{\sigma_3 - \sigma_2} \times 100$$

where σ_1 is the yield stress at the first hit, σ_2 the yield stress of the second hit, and σ_3 the stress at the end of the first hit. It should be noted that the effect introduced by static recovery cannot be distinguished from the recrystallization effect with this method. For this reason, double-hit experiment stress-strain curves combined with microstructure characterization by electron backscattered diffraction (EBSD) and/or TEM are commonly used (see Fig. 11 [91]). The degree of PDRX

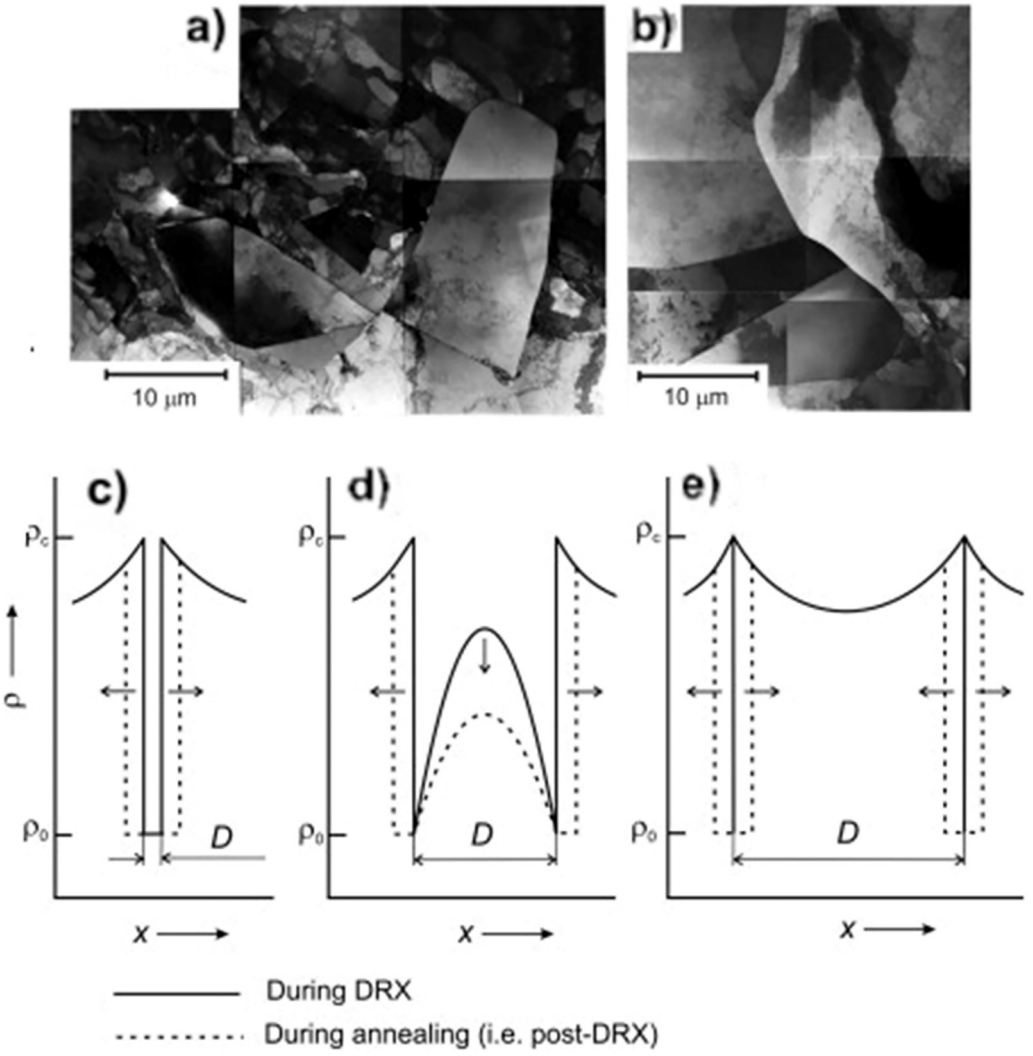

Fig. 10. TEM micrographs of DRXed nickel kept at the deformation temperature of 1050 K for a) 0.03 s, b) 10 s. Three types of dislocation density distributions develop in the microstructure, c) a DDRX nucleus, d) a growing DDRX grain, and e) a critically strain hardened DDRX grain [3].
Reproduced from [3], with permission from Elsevier.

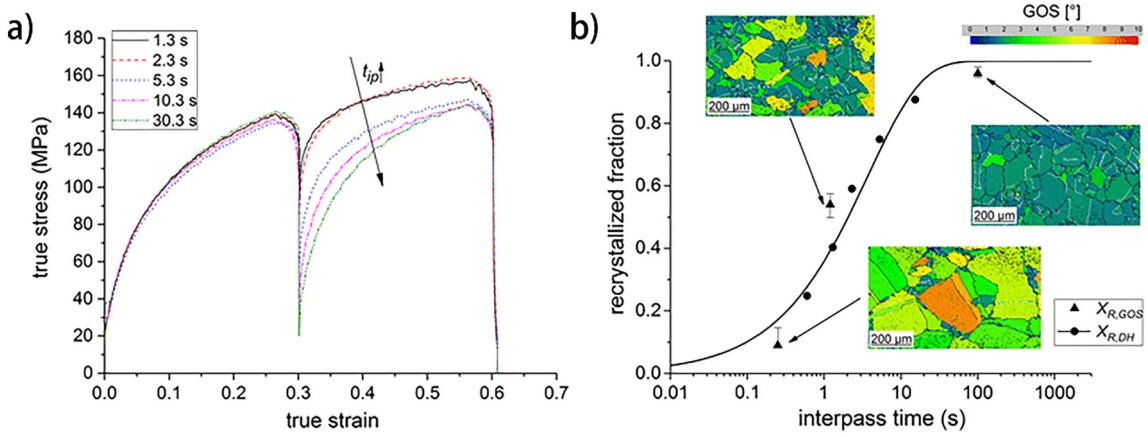

Fig. 11. Results of the double-hit compression tests carried out on C—Mn steel samples [91]. a) The true stress-strain curve of sample deformation at 915 °C, b) Austenitic microstructures according to the GOS method with the recrystallization curve determined by samples at a deformation temperature of 1000 °C.
Reprinted with permission from Springer [91].

after hot deformation can be understood more directly, but this, again, requires fast quench after hot deformation. Recently, Nicolaÿ et al. [92] reported a new approach for distinguishing PDRX grains from the DRX grains based on the analysis of intragranular misorientations in EBSD maps with enhanced angular resolution.

In order to avoid or mitigate the interference of PDRX with DRX, samples should be quenched as quickly as possible after hot deformation. Compared with the traditional practice of moving hot-deformed samples into a cooling medium, in-situ spray cooling can ensure faster quenching. Moreover, the gas quenching method can also achieve rapid cooling if appropriate gas temperature, gas pressure and gas flow rate are employed [83]. Even though the importance of timely quenching is self-evident, quench delay is usually unavoidable experimentally [93]. In fact, large workpieces are often not quenched after hot deformation during production [94], and even if they are quenched, the core of the workpiece will be cooled more slowly than the surface, i.e. the quench delay there is almost inevitable. Moreover, the low thermal conductivity of certain materials is another key factor that delays fast quenching.

If immediate quench is difficult, an effective way to avoid significant PDRX is to reduce the stain rate and/or deformation temperature during laboratory DRX studies. For example, in a coarse-grained two-phase titanium alloy, PDRX after a small strain rate ($0.01\ s^{-1}$) deformation at 1080 °C proceeds much slower than that with large strain rate ($0.1\ s^{-1}$) [95]. Similar results are also verified in 300 M steel [96] and 0.34% plain-carbon steel [90]. The temperature dependence of PDRX lies in both the number of DRX nuclei, and in their growth rate [96].

5. Phase transformation

In order to study the DRX behaviour, metallic materials are usually deformed at high temperatures, after which the deformed samples are cooled down to examine their microstructures. When the samples are cooled down from high temperatures to room temperature, phase

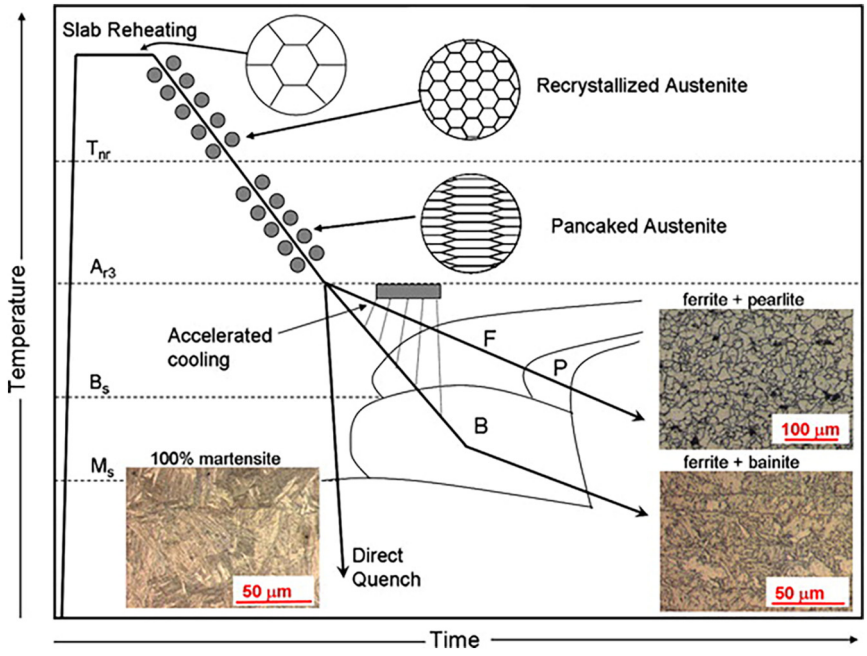

Fig. 12. Schematic diagram of thermomechanical controlled processing of HSLA steels and the different microstructures that result from this process during cooling [99].
Reproduced from [99], with permission from Taylor & Francis.

transformation can take place for many metallic materials, typical examples include steels, titanium alloys. Another less studied type of phase transformation is the strain induced phase transformation, also called dynamic transformation, during hot deformation [97], which will be discussed later. Once the different types of potential phase transformations related to hot deformation are known, it is possible to account for their disturbing effect when investigating DRX.

5.1. Static phase transformation

It is textbook knowledge that typical structural metallic materials like steels and Ti alloys usually experience phase transformation from austenite to ferrite and from bcc β to hcp α phase, respectively, when cooled from high temperatures (in austenite or β region). The addition of alloying elements can lower the transformation starting temperature and stabilize the high temperature phase, which then suppress phase transformation. For this reason, austenitic stainless steels and β-Ti alloys are often chosen as model alloys to study DRX. But for many other metallic materials such as high strength low alloy (HSLA) steels, carbon steels and α + β Ti alloys, martensitic phase transformation does take place during fast cooling, leading to a completely different microstructure than the hot deformed one, which shields many characters of the hot deformation (sub)structures [98]. The different microstructures after cooling of hot deformed HSLA steel are schematically shown in Fig. 12 [99].

As a typical type of model steel for DRX studies, austenitic stainless steel does not experience phase transformation after quick quench to room temperature. It can be seen from Fig. 13 that the hot deformation substructures in terms of LAGBs are reserved [100]. The size, volume fraction and location of DRX grains, which are all important parameters for DRX studies, are accessible for direct quantitative analysis. On the other hand, the hot deformed austenitic structures are replaced by martensite after quenching for many other steels such as advanced high strength steel 22MnB5 steel [101], as shown in Fig. 14. Quantitative analysis of the DRX behaviour is thus almost impossible, even though the prior austenite GBs can be reconstructed using the orientation relationships between martensitic and austenitic grains as will be detailed later. Even though only examples of steels are shown here, it should be noted that similar situation can also be found for other metallic materials such as Ti alloys.

Since phase transformation during cooling masks the high temperature structure, the traditional way to characterize the microstructure of the cooled samples at room temperature is not applicable. Alternative approaches have been proposed, they are summarized below.

The most straightforward way to study DRX in materials with phase transformation is by combining hot deformation with in-situ characterization techniques, including in-situ SEM-EBSD deformation [102], in-situ TEM deformation [103] or even in-situ synchrotron radiation diffraction deformation [104]. During in-situ SEM-EBSD deformation, the slow data acquisition is a major concern since small scanning step size is usually required to capture accurately enough the microstructure evolution. While this issue may be tackled with the fast development of the EBSD technique, it is more challenging to keep the scanning sample surface flat during deformation, which causes serious problems for high quality indexing. On the other hand, a very small surface area is typically analysed when dealing with in-situ TEM deformation, whereas DRX is a quite heterogeneous process-efforts must therefore be invested to ensure the right area is chosen. In practice, DRX studies by in-situ TEM are rarely reported. In both SEM-EBSD and TEM techniques, the microstructure is observed close to free surfaces, which may introduce artefacts. In contrast, no free surface effect is involved for in-situ synchrotron radiation diffraction deformation, however the data analysis procedure is complex, and often user dependent. It should be noted that DRX can also be indirectly studied by indentation at high temperature [105].

Since in-situ observation of dynamic microstructure evolution often requires special equipment, the reconstruction of the hot deformation structure from the "frozen" (room temperature) microstructure is perhaps the most widely used approach. Before the emergence of EBSD, the hot deformation structure before phase transformation was usually characterized using special etching process/agents, see Fig. 15 [106]. However, it is unclear whether all high temperature GBs can be retrieved using this method, especially when different etching recipes are used in different research groups. With more and more reliable EBSD measurements, crystallographic models [107] are able to reconstruct the hot deformation microstructure before phase transformation occurred. These models are based on orientation relationships between high and low temperature phases (typically austenite and martensite). An example of reconstructed austenite grain structure after friction stir welding is shown in Fig. 16 [108]. The hot deformation substructure (sometimes even the fine precipitates), and in particular the surrounding environment of the DRX nuclei, is however lost after the phase transformation when using these reconstruction methods.

5.2. Dynamic transformation (DT)

In general, most of laboratory studies on DRX of steels are conducted above the Ae_3 temperature but below the delta ferrite formation temperature, where austenite is the equivalent phase. Austenite can be

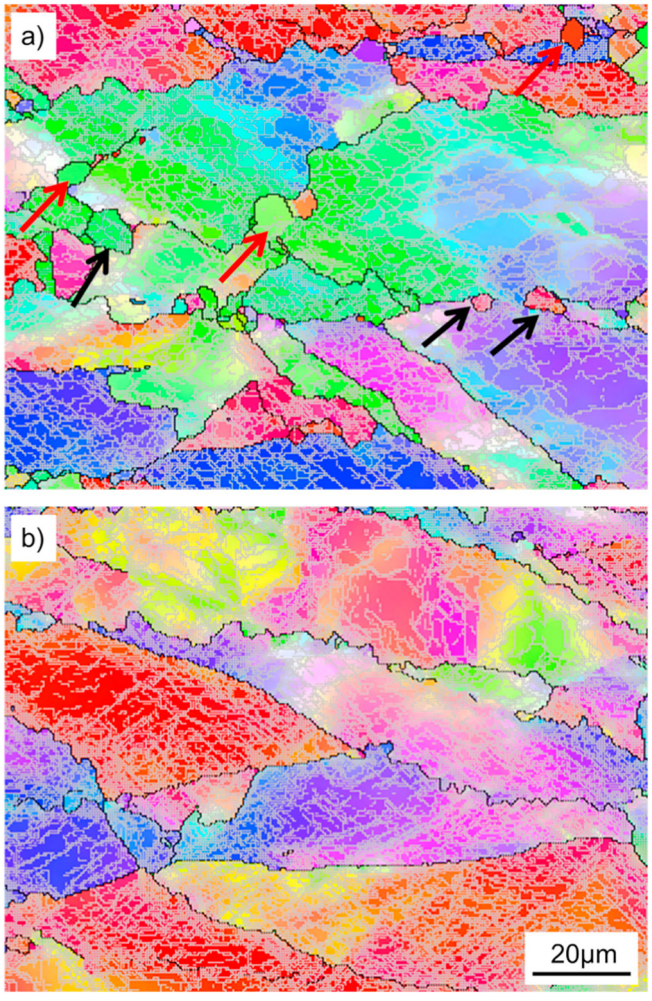

Fig. 13. EBSD micrographs showing the details of the deformed microstructure of the 304 L samples deformed at 1000 °C to ε = 0.5. Low angle grain boundaries with misorientation angle 1° < θ < 15° were plot in grey. a) 0.01 s^{-1}, b) 0.1 s^{-1} [100].
Reprinted with permission from Elsevier [100].

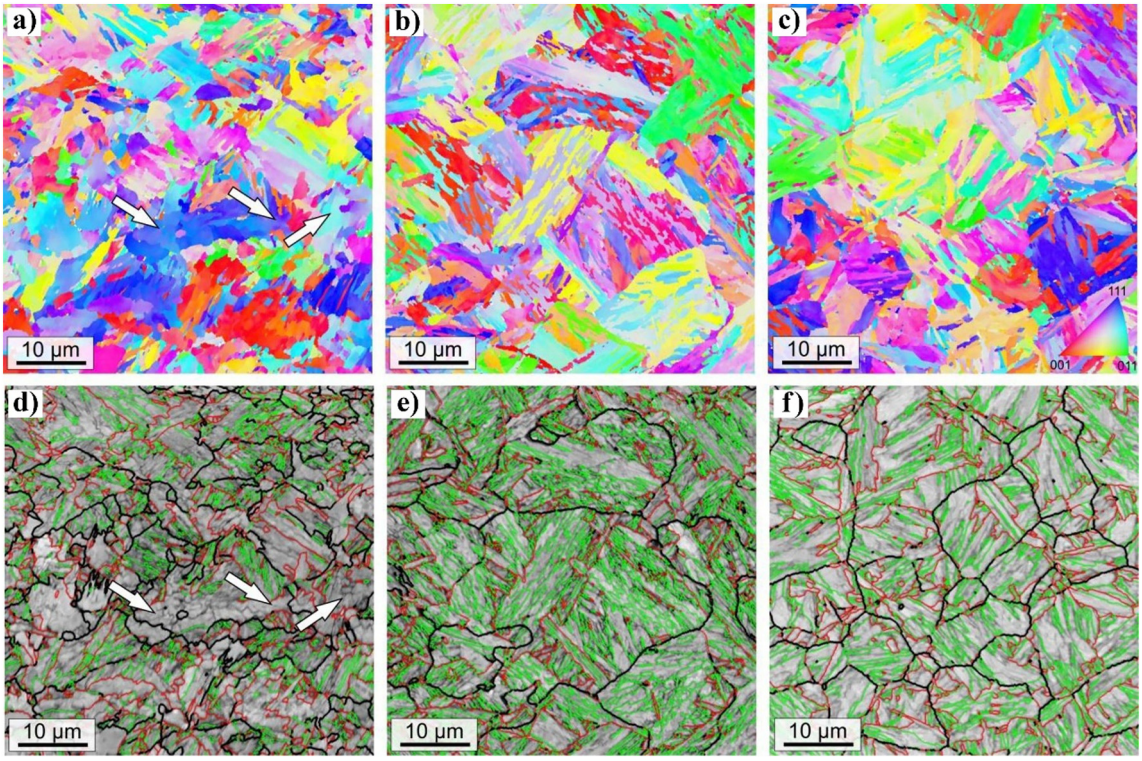

Fig. 14. The EBSD micrographs of an advanced high strength steel (22MnB5 steel) deformed to $\varepsilon = 1$ (a-c) EBSD orientation mappings (IPF color coding with respect to the sample surface) and (d-f) EBSD band contrast images superimposed with the reconstructed parent austenite grain boundaries (black lines), the packet boundaries (red lines) and block boundaries (green lines) of martensite. (a + d) 850 °C/0.01 s^{-1}, (b + e) 950 °C/0.01 s^{-1}, (c + f) 950 °C/0.8 s^{-1} [101].
Reprinted with permission from Elsevier [101].

readily transformed into ferrite during deformation between the Ae_3 and Ar_3 temperatures, however, DRX is not prevailed at this low temperature [109]. Therefore, only selected hot deformation experiments performed at temperatures above the Ae_3 are further discussed in this paper. DT, which refers to the transformation of austenite to ferrite during deformation, has been reported since 1980s in the pioneering work by Yada et al. [110]. However, the nature of the DT mode is still unclear, various transformation modes are proposed in the literature including the diffusional transformation [111,112], massive transformation [113,114], displacive transformation [115]. Meanwhile, the thermodynamics of DT have been studied using different approaches, i.e., stored energy, stress activation and transformation softening models [97]. More details on DT can be found in a recent review paper on hot deformation of steels [97]. It should be note that DT also takes place on titanium alloys [116,117], this is, however, not further discussed.

The existence of DT during hot deformation has been unambiguously proved by torsion test of Fe-6Ni-(0.0008–0.29)C alloys samples 40 °C above the Ae_3 with in-situ X-ray experiments [97,113]. It was shown from Fig. 17 that a line corresponding to $(1\,1\,0)_\alpha$ was present together with the $(1\,1\,1)_\gamma$ line. This clearly showed that $\gamma \rightarrow \alpha$ transformation occurred during deformation. More evidences were later established through EBSD, TEM and APT results [97].

Once the existence of DT during hot deformation is confirmed, its relevance to DRX can be now examined. It is now well accepted that there is a critical strain for DT below which phase transformation does not take place. The values of the critical stresses (σ_c) for the onset of DT and DRX can actually be estimated by the so-called double differentiate method [118,119] using the flow stress curve and θ vs. σ curves, where θ is the work hardening rate $\theta = (\partial\sigma/\partial\varepsilon)$. An example is presented below in Fig. 18 [97,120]. It should be noted that the critical

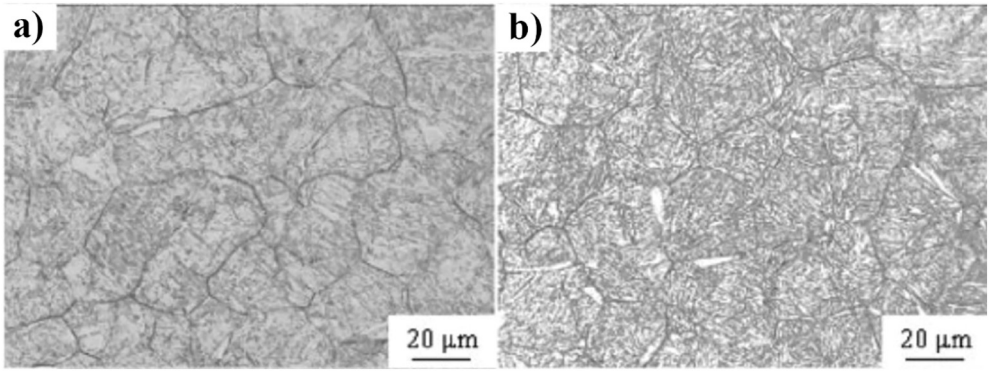

Fig. 15. Prior austenite grain boundaries are revealed by special etching agents in 300 M steel isothermal compression at a) 1180 °C and b) 1140 °C [106].
Reproduced with permission from Elsevier [106].

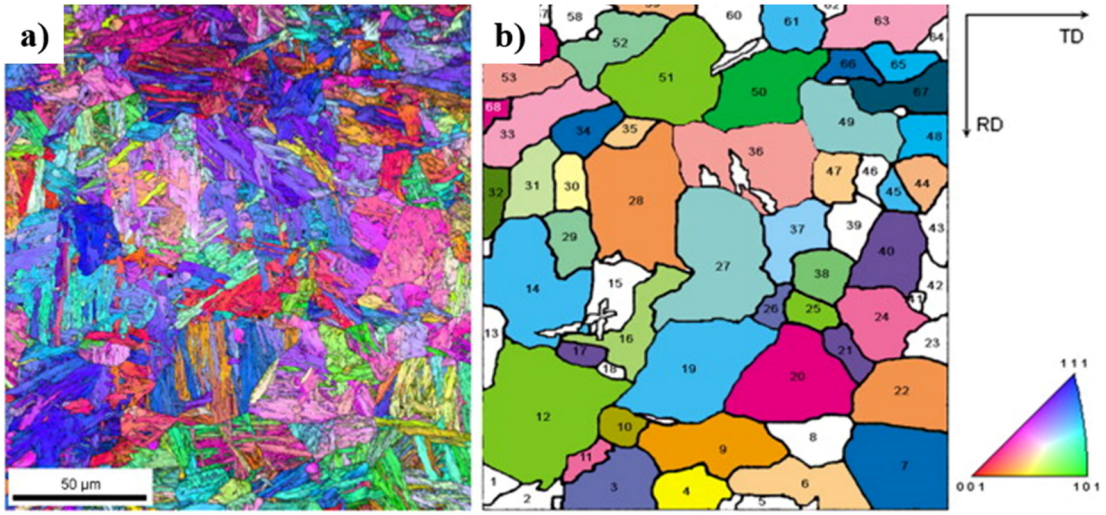

Fig. 16. Inverse pole figure map combined with image quality map of the room temperature microstructure a), and reconstructed prior austenite inverse pole figure map b) after friction stir welding of a ferritic steel (orientations of white prior austenite grains were not recoverable due to low number of active ferrite variants) [108].
Reproduced with permission from Elsevier [108].

strain for DT is always lower than that for DRX, which means DT will always take place earlier than DRX under conditions where both phenomena take place. Since DT consumes the stored energy in the original austenite phase during hot deformation, it is thus not surprising that it retards the DRX of the parent austenite phase.

The effect of deformation conditions in terms of deformation temperature and strain rate on DT and DRX is now discussed. DRX is promoted at high deformation temperatures, however, the amounts of DT ferrite decrease as the deformation temperature is increased (still below the delta ferrite temperature). This is expected since the Gibbs energy barrier to the γ-to-α transformation increases with deformation temperature. In other words, DT can be largely prohibited when studying DRX at high deformation

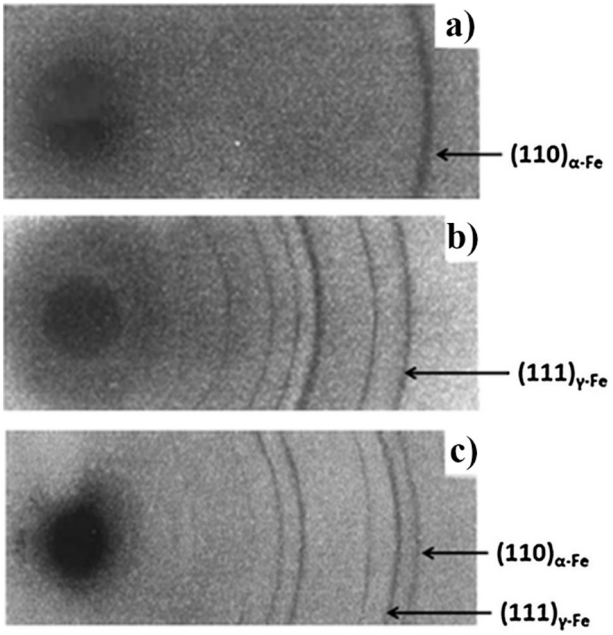

Fig. 17. Typical X-ray diffraction patterns a) before heating, b) at the austenitizing temperature (790 °C), and c) on the application of torsional deformation at 720 °C (i.e. paraequilibrium Ae_3 + 40 °C) temperature [97,113].
Reproduced with permission from Elsevier [97].

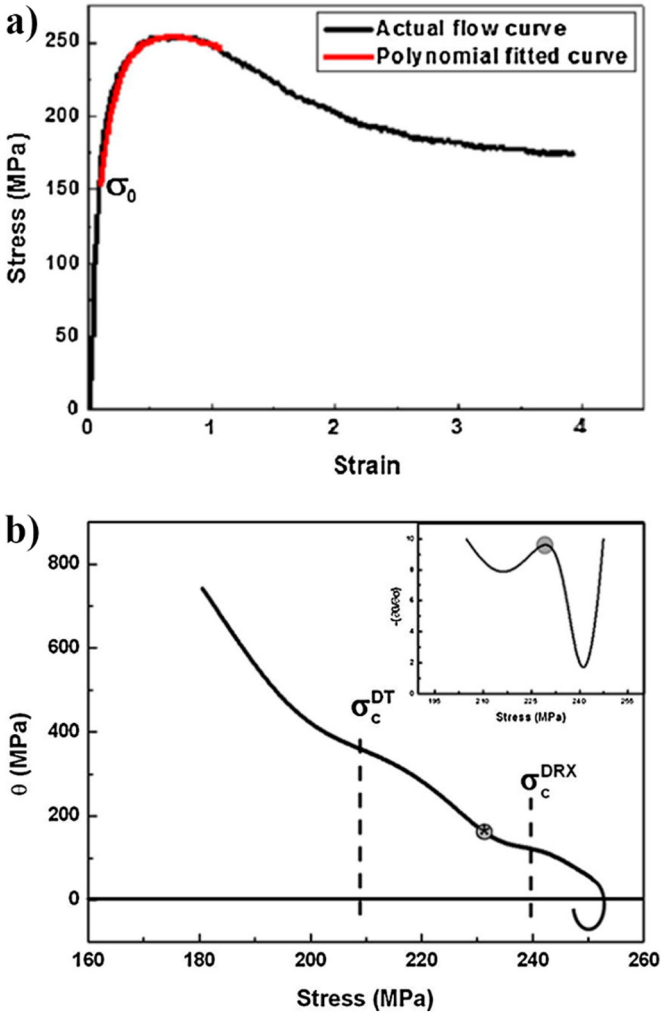

Fig. 18. a) Stress-strain curve from hot torsion on a 0.79 wt% C steel deformed at 763 °C (i.e. Ae_3 + 30 °C) at a strain rate of 4.0 s^{-1}. b) θ-σ plot derived from the fitted curve. Here the two σ_c values are associated with two of the points of inflection. The '*' on the plot corresponds to the local maximum in the inset [97,120].
Reprinted with permission from Elsevier [97].

temperatures. Lowering deformation temperature favors DT and reduces the resultant ferrite grain size, but DRX may be sluggish or even prohibited at such deformation temperature range. In terms of strain rate, lower strain rate is always preferred during DRX, but its effect on DT is twofold. On one hand, increasing strain rate retards DRX of austenite which then accumulates more stored energy to promote DT. On the other hand, larger strain rate reduces the deformation duration, which is unfavorable to DT since it is a time dependent process. The net effect of strain rate on DT thus depends on the balance of the above two factors, which provides the guidance to avoid DT by varying strain rate during DRX studies.

DT takes place by transforming the harder austenite phase to softer ferrite phase during hot working [97]. As a consequence, deformation may concentrate on the DT-ferrite, which increases the driving force for the onset of DRX in this transformed phase (not the original austenite phase since it is less deformed). Since recovery is enhanced in ferrite at elevated temperature as compared to austenite, the critical strain to initiate DRX when deforming single ferrite phase sample at relatively low temperature (in the DT temperature region) is typically very large. However, DRX of DT-ferrite occurs at a relatively small macroscopic strain because applied strain significantly concentrates on DT-ferrite [112], i.e., DT promote DRX of the transformed phase. It should be noted that the DT phase may subject to further transformation during deformation or unloading since it is metastable [97,117,121], which adds difficulty to the analysis of DRX behaviour of the parent phase.

6. Summary

In response to the typical problems encountered in experimental studies of DRX, the following topics were addressed in this paper:

1) The current misunderstandings related to the three common DRX mechanisms, i.e., DDRX, CDRX and GDRX, were discussed and clarified. New DRX mechanisms were also presented, including their application conditions and limitations.
2) Various sources of strain localization and their consequence on DRX studies were identified; specific methods to eliminate or reduce strain localization were described.
3) Phase transformation and post-dynamic recrystallization (PDRX) and, which may take place during or after hot deformation and mask the high temperature structure, are considered as key disturbing factors for DRX studies. Practical solutions to deal with such phenomena were examined.

CRediT authorship contribution statement

H.K. Zhang: Writing - original draft. **H. Xiao:** Writing - original draft. **X.W. Fang:** Formal analysis, Resources. **Q. Zhang:** Formal analysis. **R.E. Logé:** Writing - review & editing. **K. Huang:** Conceptualization, Project administration, Supervision, Writing - review & editing.

Declaration of competing interest

The authors declare that they have no known competing financial interests or personal relationships that could have appeared to influence the work reported in this paper.

Acknowledgement

The authors would like to acknowledge the financial support from the National Natural Science Foundation of China [51805415, 51875441], the Natural Science Basis Research Plan in Shaanxi Province of China [Program No. 2019JM-125], the Fundamental Research Funds for the Central Universities [xzd012019033] and the Open Research Fund of State Key Laboratory of High Performance Complex Manufacturing, Central South University [Kfkt2018-04]. RL is thankful for the financial support from PX Group.

References

[1] J. Humphreys, G. Rohrer, A. Rollett, Recrystallization and Related Annealing Phenomena 3rd edn, Elsevier, Oxford, 2017.
[2] H.J. McQueen, Mater. Sci. Eng. A 387–389 (2004) 203–208, https://doi.org/10.1016/j.msea.2004.01.064.
[3] T. Sakai, A. Belyakov, R. Kaibyshev, et al., Prog. Mater. Sci. 60 (2014) 130–207, https://doi.org/10.1016/j.pmatsci.2013.09.002.
[4] K. Huang, R.E. Logé, Mater. Des. 111 (2016) 548–574, https://doi.org/10.1016/j.matdes.2016.09.012.
[5] K. Huang, K. Marthinsen, Q.L. Zhao, et al., Prog. Mater. Sci. 92 (2018) 284–359, https://doi.org/10.1016/j.pmatsci.2017.10.004.
[6] J.J. Jonas, X. Quelennec, L. Jiang, Acta Mater. 57 (2009) 2748–2756, https://doi.org/10.1016/j.actamat.2009.02.033.
[7] H. Hallberg, Metals 1 (2011) 16–48, https://doi.org/10.3390/met1010016.
[8] H. Miura, T. Sakai, R. Mogawa, et al., Philos. Mag. 87 (2007) 4197–4209, https://doi.org/10.1080/14786430701532780.
[9] M.E. Wahabi, L. Gavard, F. Montheillet, et al., Acta Mater. 53 (2005) 4605–4612, https://doi.org/10.1016/j.actamat.2005.06.020.
[10] Z. Wan, Y. Sun, L. Hu, et al., Mater. Des. 122 (2017) 11–20, https://doi.org/10.1016/j.matdes.2017.02.088.
[11] T. Sakai, J.J. Jonas, Acta Metall. 32 (1984) 189–209, https://doi.org/10.1016/0001-6160(84)90049-X.
[12] H.J. McQueen, M.E. Kassner, Scr. Mater. 51 (2004) 461–465, https://doi.org/10.1016/j.scriptamat.2004.05.027.
[13] J. Driver, Mater. Lett. 222 (2018) 135–137, https://doi.org/10.1016/j.matlet.2018.03.196.
[14] C.H. Perdrix, M.Y. Perrin, F. Montheillet, Mem Etud Sci Rev Metall 78 (1981) 309–320.
[15] J.Ch. Gleza, J.H. Driverb, Acta Mater. 51 (2003) 2989–3003, https://doi.org/10.1016/S1359-4(03)00111-3.
[16] K. Huang, R.E. Logé, Procedia Eng 207 (2017) 25–30, https://doi.org/10.1016/j.proeng.2017.10.732.
[17] C. Kobayashi, T. Sakai, A. Belyakov, et al., Phil Mag Lett 87 (2007) 751–766, https://doi.org/10.1080/09500830701566016.
[18] T. Sakai, A. Belyakov, H. Miura, Metall Mater Trans A 39 (2008) 2206–2214, https://doi.org/10.1007/s11661-008-9556-8.
[19] O. Sitdikov, T. Sakai, H. Miura, et al., Mater. Sci. Eng. A 516 (2009) 180–188, https://doi.org/10.1016/j.msea.2009.03.037.
[20] J.K. Solberg, H.J. McQueen, N. Ryum, E. Nes, Phil Mag 60 (1989) 447–471–485.
[21] H.J. McQueen, O. Knustad, N. Ryum, et al., Scr. Mater. 19 (1985) 73–78, https://doi.org/10.1016/0036-9748(85)90268-6.
[22] O. Sitdikov, R. Kaibyshev, Mater. Trans. 42 (2001) 1928–1937, https://doi.org/10.2320/matertrans.42.1928.
[23] T. Wang, J.J. Jonas, S. Yue, Metall Mater Trans A 48 (2017) 594–600, https://doi.org/10.1007/s11661-016-3896-6.
[24] Q. Ma, B. Li, E.B. Marin, et al., Scr. Mater. 65 (2011) 823–826, https://doi.org/10.1016/j.scriptamat.2011.07.046.
[25] S.W. Xu, S. Kamado, N. Matsumoto, et al., Mater. Sci. Eng. A 527 (2009) 52–60, https://doi.org/10.1016/j.msea.2009.08.062.
[26] H. Yan, S.W. Xu, R.S. Chen, et al., Scr. Mater. 64 (2011) 141–144, https://doi.org/10.1016/j.scriptamat.2010.09.029.
[27] J.Z. Sun, M.Q. Li, H. Li, J Alloy Compd 692 (2017) 403–412, https://doi.org/10.1016/j.jallcom.2016.09.065.
[28] D.L. Yin, K.F. Zhang, G.F. Wang, et al., Mater. Sci. Eng. A 392 (2005) 320–325, https://doi.org/10.1016/j.msea.2004.09.039.
[29] M.G. Jiang, H. Yan, R.S. Chen, J Alloy Compd 650 (2015) 399–409, https://doi.org/10.1016/j.jallcom.2015.07.281.
[30] T. Al-Samman, K.D. Molodov, D.A. Molodov, et al., Acta Mater. 60 (2012) 537–545, https://doi.org/10.1016/j.actamat.2011.10.013.
[31] F. Guo, D. Zhang, H. Wu, J Alloy Compd 695 (2017) 396–403, https://doi.org/10.1016/j.jallcom.2016.10.222.
[32] S.Q. Zhu, S.P. Ringer, Acta Mater. 144 (2018) 365–375, https://doi.org/10.1016/j.actamat.2017.11.004.
[33] C. Xie, J.M. He, B.W. Zhu, Int J Plasticity 111 (2018) 211–233, https://doi.org/10.1016/j.ijplas.2018.07.017.
[34] M. Aramfard, C. Deng, Sci. Rep. 5 (2015), 14215. https://doi.org/10.1038/srep14215.
[35] A.E. Romanov, A.L. Kolesnikova, Prog. Mater. Sci. 54 (2009) 740–769, https://doi.org/10.1016/j.pmatsci.2009.03.002.
[36] M.A. Charpagne, T. Billot, J.M. Franchet, et al., J Alloy Compd 688 (2016) 685–694, https://doi.org/10.1016/j.jallcom.2016.07.240.
[37] M.A. Charpagne, P. vennÉguÈs, T. Billot, et al., J. Microsc. 263 (2016) 106–112, https://doi.org/10.1111/jmi.12380.
[38] M.A. Charpagne, T. Billot, J.M. Franchet, et al., Proceedings of the 6th International Conference on Recrystallization and Grain Growth (ReX&GG 2016), Springer, Cham. doi:https://doi.org/10.1007/978-3-319-48770-0_38.
[39] M.A. Meyers, H.R. Pak, Acta Metall. 34 (1986) 2493–2499, https://doi.org/10.1016/0001-6160(86)90152-5.

[40] M.A. Meyers, V.F. Nesterenko, J.C. LaSalvia, Mater. Sci. Eng. A 317 (2001) 204–225, https://doi.org/10.1016/S0921-5093(01)01160-1.
[41] J.A. del Valle, M.T. Pérez-Prado, O.A. Ruano, Mater. Sci. Eng. A 355 (2003) 68–78, https://doi.org/10.1016/S0921-5093(03)00043-1.
[42] H. Miura, T. Sakai, R. Mogawa, et al., Scr. Mater. 51 (2004) 671–675, https://doi.org/10.1016/j.scriptamat.2004.06.015.
[43] M.F. Varzaneh, A.Z. Hanzaki, H. Beladi, et al., Mater. Sci. Eng. A 456 (2007) 52–57, https://doi.org/10.1016/j.msea.2006.11.095.
[44] R. Kaibyshev, A. Galiev, O. Sitdikov, Nanostruct. Mater. 6 (1995) 621–624, https://doi.org/10.1016/0965-9773(95)00135-2.
[45] A. Galiyev, R. Kaibyshev, G. Gottstein, Acta Mater. 49 (2001) 1199–1207, https://doi.org/10.1016/S1359-6454(01)00020-9.
[46] K.H. Wang, G. Liu, W. Tao, et al., Mater. Charact. 126 (2017) 57–63, https://doi.org/10.1016/j.matchar.2017.01.030.
[47] B. Derby, Acta Metall. 39 (1991) 955–962, https://doi.org/10.1016/0956-7151(91)90295-C.
[48] N. Dudova, A. Belyakov, T. Sakai, et al., Acta Mater. 58 (2010) 3624–3632, https://doi.org/10.1016/j.actamat.2010.02.032.
[49] D. Li, Q. Guo, S. Guo, et al., Mater. Des. 32 (2011) 696–705, https://doi.org/10.1016/j.matdes.2010.07.040.
[50] Y. Lin, X. Wu, X. Chen, et al., J Alloy Compd 640 (2015) 101–113, https://doi.org/10.1016/j.jallcom.2015.04.008.
[51] A.G. Beer, M.R. Barnett, Metall Mater Trans A 38 (2007) 1856–1867, https://doi.org/10.1007/s11661-007-9207-5.
[52] Z. Yanushkevich, A. Belyakov, R. Kaibyshev, Acta Mater. 82 (2015) 244–254, https://doi.org/10.1016/j.actamat.2014.09.023.
[53] C. Castan, F. Montheillet, A. Perlade, Scr. Mater. 68 (2013) 360–364, https://doi.org/10.1016/j.scriptamat.2012.07.037.
[54] S. Sarkar, A. Moreau, M. Militzer, et al., Metall Mater Trans A 39 (2008) 897–907, https://doi.org/10.1007/s11661-007-9461-6.
[55] D.C. Yubero, Z. Kovács, J.F.T.S. Fotso, et al., J Alloy Compd 822 (2020) 153282, https://doi.org/10.1016/j.jallcom.2019.153282.
[56] Y. Huang, F.J. Humphreys, I. Brough, J. Microsc. 208 (2002) 18–23, https://doi.org/10.1046/j.1365-2818.2002.01061.x.
[57] D. Ponge, G. Gottstein, Acta Mater. 46 (1998) 69–80, https://doi.org/10.1016/S1359-6454(97)00233-4.
[58] D. Janda, H.G. Armaki, E. Bruder, et al., Acta Mater. 103 (2016) 909–918, https://doi.org/10.1016/j.actamat.2015.11.002.
[59] J.N. Johnson, J. Appl. Phys. 52 (1981) 2812, https://doi.org/10.1063/1.329011.
[60] X. Ye, X. Gong, B. Yang, et al., T Nonferr Metal Soc 29 (2019) 279–286, https://doi.org/10.1016/S1003-6326(19)64937-X.
[61] R.W. Evans, P.J. Scharning, Mater Sci Tech 17 (2001) 995–1004, https://doi.org/10.1179/026708301101510843.
[62] J.J. Jonas, R.A. Holt, C.E. Coleman, Acta Metall. 24 (1976) 911–918, https://doi.org/10.1016/0001-6160(76)90039-0.
[63] J.J. Jonas, B. Baldelet, Acta Metall. 25 (1977) 43–50, https://doi.org/10.1016/0001-6160(77)90244-9.
[64] D. Lunt, T. Busolo, X. Xu, et al., Acta Mater. 129 (2017) 72–82, https://doi.org/10.1016/j.actamat.2017.02.068.
[65] D. Lunt, X. Xu, T. Busolo, et al., Scr. Mater. 145 (2018) 45–49, https://doi.org/10.1016/j.scriptamat.2017.10.012.
[66] G. Lutjering, S. Weissmann, Acta Metall. 18 (1970) 785–795, https://doi.org/10.1016/0001-6160(70)90043-X.
[67] X. Hong, A. Godfrey, W. Liu, et al., Mater. Lett. 209 (2017) 94–96, https://doi.org/10.1016/j.matlet.2017.07.077.
[68] L. Li, P. Zhang, Z. Zhang, et al., Acta Mater. 73 (2014) 167–176, https://doi.org/10.1016/j.actamat.2014.04.004.
[69] J.C. Stinville, N. Vanderesse, F. Bridier, et al., Acta Mater. 98 (2015) 29–42, https://doi.org/10.1016/j.actamat.2015.07.016.
[70] J.C. Stinville, M.P. Echlin, D. Texier, Exp. Mech. 56 (2015) 197–216, https://doi.org/10.1007/s11340-015-0083-4.
[71] F.D. Gioacchino, J.Q. da Fonseca, Int J Plasticity 74 (2015) 92–109, https://doi.org/10.1016/j.ijplas.2015.05.012.
[72] S. Khoddam, H. Beladi, P.D. Hodgson, Mater. Des. 60 (2014) 146–152, https://doi.org/10.1016/j.matdes.2014.03.063.
[73] M.F. Ashby, Engineering Materials. An Introduction to Microstructures, Processing and Design, Elsevier, Oxford, 2006.
[74] A.O. Caballero, D. Lunt, J.D. Robson, et al., Acta Mater. 133 (2017) 367–379, https://doi.org/10.1016/j.actamat.2017.05.040.
[75] A.D. Kammers, S. Daly, Exp. Mech. 53 (2013) 1743–1761, https://doi.org/10.1007/s11340-013-9782-x.
[76] C. Fressengeas, A. Molinari, Acta Metall. 33 (1985) 387–396, https://doi.org/10.1016/0001-6160(85)90081-1.
[77] F.J. Zhu, H.Y. Wu, M.C. Lin, et al., J. Mater. Eng. Perform. 24 (2015) 2051–2059, https://doi.org/10.1007/s11665-015-1474-5.
[78] X. Zhou, K.L. Wang, S.Q. Lu, et al., J Mater Res Technol (2020)https://doi.org/10.1016/j.jmrt.2019.12.093.
[79] S.D. Antolovich, R.W. Armstrong, Prog. Mater. Sci. 59 (2014) 1–160, https://doi.org/10.1016/j.pmatsci.2013.06.001.
[80] H. Wu, G. Fan, Prog. Mater. Sci. (2020)https://doi.org/10.1016/j.pmatsci.2020.100675.
[81] S.B. Brown, K.H. Kim, L. Anand, Int J Plasticity 5 (1989) 95–130, https://doi.org/10.1016/0749-6419(89)90025-9.
[82] R.A.P. Djaic, J.J. Jonas, Metall Trans 4 (1973) 621–624, https://doi.org/10.1007/bf02648720.
[83] T. Sakai, M. Ohashi, K. Chiba, et al., Acta Metall. 36 (1988) 1781–1790, https://doi.org/10.1016/0001-6160(88)90246-5.
[84] A.D. Manshadi, M.R. Barnett, P.D. Hodgson, Mater. Sci. Eng. A 485 (2008) 664–672, https://doi.org/10.1016/j.msea.2007.08.026.
[85] Y.C. Lin, M.S. Chen, Mater. Sci. Eng. A 501 (2009) 229–234, https://doi.org/10.1016/j.msea.2008.10.003.
[86] H. Beladi, P. Cizek, P.D. Hodgson, Scr. Mater. 62 (2010) 191–194, https://doi.org/10.1016/j.scriptamat.2009.10.022.
[87] O. Beltran, K. Huang, R.E. Logé, Comput. Mater. Sci. 102 (2015) 293–303, https://doi.org/10.1016/j.commatsci.2015.02.043.
[88] Y.C. Lin, L.T. Li, Y.C. Xia, Comput. Mater. Sci. 50 (2011) 2038–2043, https://doi.org/10.1016/j.commatsci.2011.02.004.
[89] M. Zouari, R.E. Logé, N. Bozzolo, Metals 7 (2017) 476, https://doi.org/10.3390/met7110476.
[90] K.P. Rao, Y.K.D.V. Prasad, E.B. Hawbolt, J Mater Process Tech 77 (1998) 166–174, https://doi.org/10.1016/S0924-0136(97)00414-7.
[91] T. Kramer, L. Eisenhut, L. Germain, et al., Metall Mater Trans A 49 (2018) 2759–2802, https://doi.org/10.1007/s11661-018-4593-4.
[92] A. Nicolaÿ, G. Fiorucci, J.M. Franchet, Acta Mater. 174 (2019) 406–417, https://doi.org/10.1016/j.actamat.2019.05.061.
[93] M. Zouari, N. Bozzolo, R.E. Logé, Mater. Sci. Eng. A 655 (2016) 408–424, https://doi.org/10.1016/j.msea.2015.12.102.
[94] S. Yuan, X. Fan, Int J Extrem Manuf 1 (2019), 022002. https://doi.org/10.1088/2631-7990/ab22a9.
[95] X. Fan, H. Yang, P.F. Gao, et al., J Mater Process Tech 234 (2016) 290–299, https://doi.org/10.1016/j.jmatprotec.2016.03.031.
[96] J. Liu, Y. Liu, H. Lin, et al., Mater. Sci. Eng. A 565 (2013) 126–131, https://doi.org/10.1016/j.msea.2012.11.116.
[97] C. Ghosh, C. Aranas Jr., J.J. Jonas, Prog. Mater. Sci. 82 (2016) 151–233, https://doi.org/10.1016/j.pmatsci.2016.04.004.
[98] L. Lan, W. Zhou, R.D.K. Misra, Mater. Sci. Eng. A 756 (2019) 18–26, https://doi.org/10.1016/j.msea.2019.04.039.
[99] S. Vervynckt, K. Verbeken, B. Lopez, et al., Int. Mater. Rev. 57 (2012) 187–207, https://doi.org/10.1179/1743280411Y.0000000013.
[100] K. Huang, R.E. Logé, Mater. Sci. Eng. A 711 (2018) 600–610, https://doi.org/10.1016/j.msea.2017.11.042.
[101] Y.K. Xu, P. Birnbaum, S. Pilz, et al., Results Phys 14 (2019), 102426. https://doi.org/10.1016/j.rinp.2019.102426.
[102] S.I. Wright, M.N. Nowell, Electron Backscatter Diffraction in Materials Science, Springer, 2009 329–337, https://doi.org/10.1007/978-0-387-88136-2_24.
[103] W. Kang, M. Merrill, J.M. Wheeler, Nanoscale 9 (2017) 2666–2688, https://doi.org/10.1039/C6NR07330A.
[104] R.H. Buzolin, C.L. Mendis, D. Tolnai, Mater. Sci. Eng. A 664 (2016) 2–9, https://doi.org/10.1016/j.msea.2016.03.121.
[105] J.M. Wheeler, C. Niederberger, C. Tessarek, Int. J. Plast. 40 (2013) 140–151, https://doi.org/10.1016/j.ijplas.2012.08.001.
[106] J. Luo, M.Q. Li, Y.G. Liu, et al., Mater. Sci. Eng. A 534 (2012) 314–322, https://doi.org/10.1016/j.msea.2011.11.075.
[107] C. Cayron, J Appl Crystallgr 40 (2007) 1183–1188, https://doi.org/10.1107/S0021889807048777.
[108] M. Abbasi, T.W. Nelson, C.D. Sorensen, et al., Mater. Charact. 66 (2012) 1–8, https://doi.org/10.1016/j.matchar.2012.01.010.
[109] H. Beladi, G.L. Kelly, A. Shokouhi, et al., Mater. Sci. Eng. A 371 (2004) 343–352, https://doi.org/10.1016/j.msea.2003.12.024.
[110] H. Yada, Y. Matsumura, T. Senuma, Proceedings of the international conference on martensitic transformation, JIM (1986) 515–520.
[111] H. Beladi, G.L. Kelly, P.D. Hodgson, Int. Mater. Rev. 52 (2007) 14–28, https://doi.org/10.1179/174328006X102538.
[112] A. Shibata, Y. Takeda, N. Park, et al., Scr. Mater. 165 (2019) 44–49, https://doi.org/10.1016/j.scriptamat.2019.02.017.
[113] H. Yada, C.M. Li, H. Yamagata, ISIJ Int. 40 (2000) 200–206, https://doi.org/10.2355/isijinternational.40.200.
[114] J.K. Park, K.H. Kim, J.H. Chung, et al., Metall Mater Trans A 39 (2008) 235–242, https://doi.org/10.1007/s11661-007-9404-2.
[115] C. Ghosh, V.V. Basabe, J.J. Jonas, Acta Mater. 61 (2013) 2348–2362, https://doi.org/10.1016/j.actamat.2013.01.006.
[116] J.J. Jonas, C. Aranas Jr., A. Fall, et al., Mater. Des. 113 (2017) 305–310, https://doi.org/10.1016/j.matdes.2016.10.039.
[117] X.K. Ji, B.Q. Guo, F.L. Jiang, et al., J Mater Sci Tech 36 (2020) 160–166, https://doi.org/10.1016/j.jmst.2019.08.005.
[118] E.I. Poliak, J.J. Jonas, Acta Mater. 44 (1996) 127–136, https://doi.org/10.1016/1359-6454(95)00146-7.
[119] C. Ghosh, V.V. Basabe, J.J. Jonas, Steel Res Int 84 (2013) 490–494, https://doi.org/10.1002/srin.201200188.
[120] C. Ghosh, Ph.D. thesis. McGill University, Montreal, Canada, 2013.
[121] B.Q. Guo, S.L. Semiatin, J.J. Jonas, et al., J. Mater. Sci. 53 (2018) 9305–9315, https://doi.org/10.1007/s10853-018-2237-0.